WAVES AND TIDES IN COASTAL PROCESSES

By Arthur T. Ippen*

(Presented as one of the John R. Freeman Lectures on Fundamental Hydraulic Processes in Water Resources Engineering, Fall, 1963.)

Introduction

It is naturally impossible to compress the broad developments of water-wave theory and of the related laboratory and field observations on wave phenomena into a manageable presentation in a few pages. The task of this presentation on coastal phenomena has therefore been conceived as one to give a first basis of the elements of wave theory in order to establish certain definitions as a means of communication and then to concentrate on some of the tidal phenomena of primary engineering interest in recent years. It is in the latter phase that certain contributions to knowledge have originated from the author and some of his colleagues, thus providing the personal relation to the material, which hopefully will enhance this presentation.

A. Principles of Wave Motion—Auxiliary Notes

1. *Properties of Single Wave Trains*

As a first approximation water-wave motion is described by the "small amplitude wave theory." This is the classical approach extremely useful in many engineering problems, but failing in others, such as the breaking of waves, which must be described by more refined "finite amplitude" approaches. The basic assumptions of the "small amplitude" theory are those inherent generally in irrotational motion and in addition, that all motions are small enough so that terms containing the squares of velocities may be neglected in the equations of motion. The available equations are therefore for the unsteady motion considered, with density constant throughout:

$$-\frac{\partial \phi}{\partial t}+\frac{p}{\rho}+gz=0 \qquad (1)$$

derived from Newton's law, and:

* Professor of Civil Engineering, Hydrodynamics Laboratory, Massachusetts Institute of Technology, Cambridge 39, Massachusetts.

$$\frac{du}{\partial x} + \frac{\partial w}{\partial z} = 0 = -\left(\frac{\partial^2 \phi}{\partial x^2} + \frac{\partial^2 \phi}{\partial z^2}\right) \tag{2}$$

derived from continuity.

The introduction of the velocity potential ϕ has reduced the number of variables by one, since $u = -\frac{\partial \phi}{\partial x}$ and $w = -\frac{\partial \phi}{\partial z}$ by definition.

With appropriate boundary conditions these equations can be solved:

$$\text{at the surface, where } \frac{p}{\rho} = 0 : \eta = \frac{1}{g}\left(\frac{\partial \phi}{\partial t}\right) t = \eta$$

$$\text{at the bottom, where } z = -h : w = -\frac{\partial \phi}{\partial z} = 0$$

The periodic solutions with the notations of Fig. 1a are:

$$\text{for the surface: } \eta = a \sin (kx - \sigma t) \tag{3}$$

$$\text{for the pressure at any depth: } \frac{p}{\gamma} = \eta \frac{\cosh k(h+z)}{\cosh k\, h} - z \tag{4}$$

$$\text{for the velocity } u : u = \frac{a\, g\, k}{\sigma} \frac{\cosh k(h+z)}{\cosh k\, h} \sin (k\, x - \sigma t) \tag{5}$$

$$w = \frac{a\, g\, k}{\sigma} \frac{\sinh k(h+z)}{\cosh k\, h} \cos (k\, x - \sigma t) \tag{6}$$

wherein:

$k = \frac{2\pi}{L}$ the "wave number"

$\sigma = \frac{2\pi}{T}$ the "wave frequency"

hence:

$\frac{\sigma}{k} = \frac{L}{T} = C$ the "wave velocity" as the ratio of wave length L to wave period T.

The most important implications of these particular solutions may be summarized as follows:

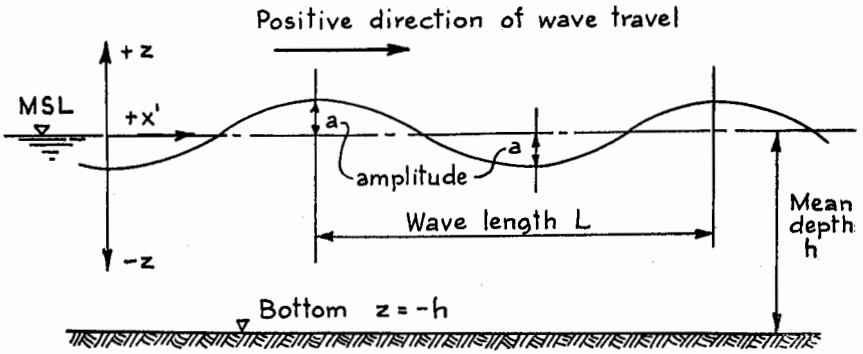

FIG. 1a.—SMALL AMPLITUDE WAVE NOTATIONS

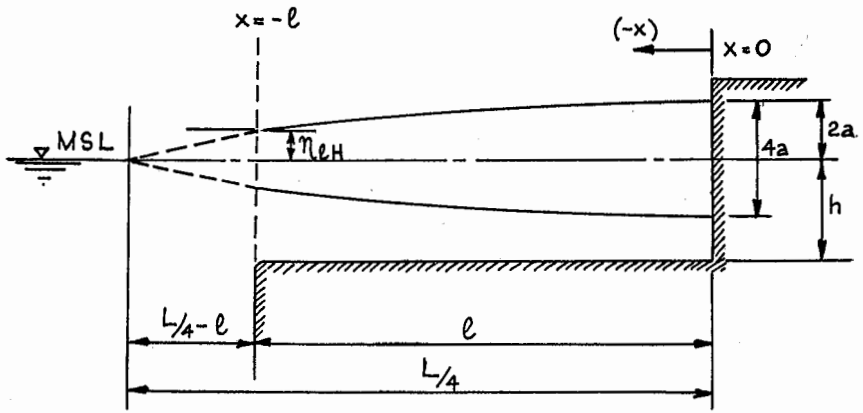

FIG. 1b.—STANDING WAVE IN CHANNEL OF LENGTH LESS THAN ONE QUARTER WAVE LENGTH

1.1 The *wave profile:* $\eta = a \sin (ks - \sigma t)$ represents a periodic variation of the surface at any given station x between the limits $+a$ and $-a$ for time intervals equal to the wave period. The same amplitude η is present at the same instant of time at all stations $(x + nL)$ wherein $n = 1, 2, 3, \ldots\ldots$

1.2 If we move along with the wave speed, i.e., we are attaching ourselves to a point so that $\eta = \text{const.}$, then $(kx - \sigma t) = \text{constant}$.

Hence:

$$x = \frac{\sigma}{k} t + \text{const.}$$

$$\frac{dx}{dt} = C = \frac{\sigma}{k} = \frac{L}{T}$$

The wave velocity is in the positive x direction and the profile represents a *"progressive wave"* moving to the right. Consequently, a progressive wave moving in the opposite direction is obtained simply by reversing the sign of σt, i.e.,

$$\eta = a \sin (kx + \sigma t)$$

1.3 A general expression for the *wave velocity C* is obtained from the equations by observing that the vertical velocity component w at the surface ($z = 0$) is approximately equal to $\partial\eta/\partial t$. This results in:

$$C = \sqrt{gh}\left(\frac{\tanh k\,h}{k\,h}\right)^{1/2} \tag{7}$$

or

$$C = \sqrt{\frac{gL}{2\pi}}\left(\tanh \frac{2\pi h}{L}\right)^{1/2} \tag{8}$$

For depths h in excess of one-half of wave length L $\left(\frac{h}{L} > 1/2\right)$ the hyperbolic tangent is close to unity and the velocity of *"deep water waves"* is obtained:

$$C_* = \sqrt{\frac{gL}{2\pi}} \tag{9}$$

For small depths h of the order of 5% of wave length L the hyperbolic tangent assumes the value of k h and the velocity of *"shallow water waves"* results:

$$C_o = \sqrt{gh} \tag{10}$$

1.4 The *wave length* generally can be derived from equation (8) when the wave period is known, since $C = \frac{L}{T}$

$$L = \frac{gT^2}{2\pi} \tanh \frac{2\pi h}{L} \tag{11}$$

For given depths, however, this equation must be solved by trial or reference to wave tables.

$$\text{For "deep water" conditions : } L_* = \frac{gT^2}{2\pi} = 5.12\ T^2 \qquad (12)$$

$$\text{and for "shallow water"} \quad : L_o = T\sqrt{gh} \qquad (13)$$

1.5 The *paths of individual fluid particles* as a wave passes may be derived by integration with time of equations (5) and (6). The total orbit of a particle is described generally by an ellipse of horizontal axis 2A and of vertical axis 2B, which are given by:

$$A = a\frac{\cosh k(h+z)}{\sinh k\,h} \qquad (14)$$

$$B = a\frac{\sinh k(h+z)}{\sinh k\,h} \qquad (15)$$

It is of interest to note that for *deep water* waves (see definition under 1.3) with good approximation:

$$A = B = a\,e^{kz} \qquad (16)$$

which indicates circular orbits of exponentially decreasing amplitude.

For *shallow water waves,* however:

$$A = a\frac{1}{k\,h} = a\frac{L}{2\pi h} \qquad (17a)$$

$$B = a\frac{k(h+z)}{k\,h} = a\left(1+\frac{z}{h}\right) \qquad (17b)$$

The maximum horizontal "excursion" of a water particle regardless of its vertical location is therefore in shallow water:

$$2A = \frac{1}{\pi}\left(\frac{a}{h}\right)L \qquad (18)$$

1.6 The *horizontal velocity u* is seen to be "in phase" with amplitude η, velocities are positive for positive values of η and vice versa.

For *shallow water waves* equation (5) reduces to:

$$u = \frac{a\,g\,k}{\sigma}\sin(kx - \sigma t)$$

with equation (10)

$$u = \frac{a}{h} C_o \sin (kx - \sigma t) \tag{19}$$

Maximum velocities are therefore quickly computed from:

$$u_o = \frac{a}{h} C_o$$

1.7 The total *energy of a wave* can be obtained from the potential and kinetic energies integrated over the depth and over a wave length utilizing equations (3) to (6). The result, expressed as average energy per unit surface area, is:

$$E = PE + KE = \gamma \frac{a^2}{4} + \gamma \frac{a^2}{4} = \gamma \frac{a^2}{2} \tag{20}$$

1.8 Through developments beyond the scope of this review it can be shown that energy is propagated at a velocity less than the wave or phase velocity C given by equation (8). This so-called *"group velocity"* C_G has a minimum value of 1/2 C in deep water and approaches C for shallow water waves. It is expressed as a function of depth and wave number:

$$C_G = C \frac{1}{2} \left(1 + \frac{2kh}{\sinh 2kh} \right) \tag{21}$$

2. *Superposition of Waves*

Waves given by the harmonic expressions in the preceding section can be superimposed and complex waves may be built up by this process. As a corollary, complex systems of waves observed in nature may be analyzed by determining the harmonic components, differing in frequency, amplitude and phase angles. This superposition applies to amplitudes, pressures and velocities, however to wave energies only under special conditions.

2.1 Waves traveling in the same direction usually at different velocities will give rise to amplification and to interference, as waves move through each other. A few simple systems may be presented for illustration:

a. Two waves of amplitudes a_1 and a_2 of the same frequency with a difference in phase δ will be given by:

$$\eta_{tot.} = a_1 \sin (k\,x - \sigma t) + a_2 \sin (k\,x - \sigma t + \delta) \qquad (22)$$

if $\delta = 0$: wave will be amplified and

$$\eta_{tot.} = (a_1 + a_2) \sin (kx - \sigma t)$$

if $\delta = 180°$: wave will be decreased by interference and

$$\eta_{tot.} = (a_1 - a_2) \sin (kx - \sigma t)$$

if $\delta = 90°$: wave will be intermediate and

$$\eta_{tot.} = a_1 \sin (kx - \sigma t) + a_2 \cos (kx - \sigma t)$$

b. Two waves traveling in the same direction, but having different amplitudes a_1 and a_2 *and* different frequencies σ_1 and σ_2, thus

$$\eta_{tot.} = a_1 \sin (k_1\,x - \sigma_1 t + \delta_1) + a_2 \sin (k_2\,x - \sigma_2 t + \delta_2)$$

The resulting wave is not harmonic, but periodic since it is readily seen that after a certain time interval T_b the same relative constellation of the waves must recur. This time is given by:

$$T_b = \frac{2\pi}{\sigma_2 - \sigma_1} = \frac{T_2\,T_1}{T_1 - T_2} \qquad (23)$$

An envelope drawn of the maximum values of $\eta_{tot.}$ shows no zero values for $(\eta_{tot.})_{max}$ and the phenomenon is known as an "incomplete beat." However, this so-called *"beat effect"* becomes very pronounced when we let the amplitudes a_1 and a_2 become equal and the frequency difference $(\sigma_2 - \sigma_1)$ become very small. In this case equation (22) can be reduced to:

$$\eta_{tot.} = 2a \cos \left(\frac{\sigma_2 - \sigma_1}{2}\right) t \sin \left(\frac{\sigma_2 + \sigma_1}{2}\right) t \qquad (24)$$

It is seen that maximum values of $\eta_{tot.}$ vary from 0 to 2a as the cosine term slowly changes with the small differential frequency, while the sine term passes through many cycles with the basic frequency $\frac{\sigma_2 + \sigma_1}{2}$. Values of $\eta_{(tot.)max.} = 0$ represent the nodic points of the beat.

2.2 One of the most important aspects of shore line structures is their property of *wave reflection* to various degrees. Such reflection also occurs at steep changes of the bottom elevation or by channel contraction. In the simplest case we may assume here for illustration that a wave of amplitude a_1, is partly reflected by a vertical barrier,

thus that the reflected wave has an amplitude a_2. The two waves may then be given by:

$$\eta_{tot.} = a_1 \sin (kx - \sigma t) + a_2 \sin (kx + \sigma t) \qquad (25)$$

adding and subtracting $a_1 \sin (kx + \sigma t)$:

$$\eta_{tot.} = 2\, a_1 \sin k\, x \cos \sigma t - (a_1 - a_2) \sin (kx + \sigma t) \qquad (26)$$

representing a progressive wave of amplitude $(a_1 - a_2)$ being reflected plus a standing wave of amplitude $2\ a_1$. Equation (25) can also be resolved into the alternate form:

$$\eta_{tot.} = (a_1 + a_2) \sin kx \cos \sigma t - (a_1 - a_2) \cos kx \sin \sigma t \qquad (27)$$

This latter form represents 2 standing waves, however, with nodal points displaced by $kx = \frac{\pi}{2}$. Therefore the envelope of the combined system must pass through $(a_1 + a_2)$ maxima and $(a_1 - a_2)$ minima, which remain fixed with respect to x. When $a_1 = a_2$ a single standing wave results from either equation (26) or (27) and the envelope shows maximum amplitudes 2 a at the anti-nodes and zero amplitudes at the nodal points, characteristic of the *true standing waves* (see Fig. 1b).

It can readily be shown that horizontal velocity components, u, reach maximum values under the nodes and are zero at the antinodes, while vertical velocities, w, are reversed in this respect.

It is clear that u and w retain finite values if a_1 is not equal to a_2.

2.3 *Reflection* phenomena in the general case become rather complex and are not completely resolved theoretically. Hence experimental evidence must be depended upon in many cases. For a barrier partly reflecting an incoming wave a_1, however, the preceding may be used to define a reflection coefficient K_r from the wave envelope as indicated by equations (25) to (27). Considering no energy loss at the reflection point and requiring that the sum of incoming wave amplitude $a_1 = a_i$ and of reflected wave amplitude $a_2 = a_r$ be equal to the transmitted wave amplitude a_t the reflection coefficient becomes:

$$K_r = \frac{a_2}{a_1} = \frac{a_r}{a_i} \qquad (28)$$

and the transmission coefficient is defined as:

$$K_t = \frac{a_t}{a_i} = 1 + K_r \tag{29}$$

When $a_2 = a_1$ obviously $K_r = 1$, when $a_2 < a_1$ these amplitudes may be determined from the fixed amplitude envelope giving $(a_1 + a_2)$ and $(a_1 - a_2)$.

3. *Transformation of Wave Properties*

Inherent in the fundamental properties of waves discussed under sections 1 and 2 are the tools by which changes in the character of wave systems may be analyzed. Implicit in equation (8) for the wave velocity, for example, is the fact that long waves will "outrun" shorter waves. From a storm-generated random wave system over the ocean after a long distance the long waves will become segregated and with little damping arrive first near the shores. With the effect of depth becoming pronounced these waves will tend to assume smaller angles relative to the shore line, their lengths will decrease and their amplitudes will increase, as they transform from deep water to shallow water waves. This refraction process can be followed by methods derived from the equations with various refinements considering the simultaneous damping by internal and especially boundary resistance. When waves encounter barriers or are of limited extent transverse to their direction of travel, energy is dispersed laterally or *diffracted.* For further discussion of wave-decay, diffraction, refraction and reflection the extensive literature must be consulted. In the following discussion more will be said about these problems in relation to their bearing on beach processes. For the present, therefore, the discussion will be centered more on the properties of very long waves in shallow water with particular emphasis on tidal waves.

3.1 Transformation *without change of energy* (2). Assuming initially no energy loss and no reflection, the rate of energy transmission is readily obtained from the product of equations (20) and (21). Considering in addition the possible variation in width B of the confining boundaries between station (0) and station (x) along the direction of travel:

$$B_o E_o C_{G_o} = B_x E_x C_{G_x}$$

or

$$B_o a_o^2 C_{G_o} = B_x a_x^2 C_{G_x} \tag{30}$$

For shallow water waves the wave velocity $C = \sqrt{gh}$ will be equal to the group velocity C_G. Hence, equation (30) may be reduced to the so-called Green's Law:

$$\frac{a_x}{a_o} = \left(\frac{B_o}{B_x}\right)^{1/2} \left(\frac{h_o}{h_x}\right)^{1/4} \tag{31}$$

which holds strictly, however, only if the reach of the gradual transition is larger than the wave length. It is seen that amplitudes increase with decreasing depth and hence decreasing wave length, while decreasing width affects amplitudes even stronger. As high amplitudes are attained the "small amplitude" theory must give way to the more appropriate, but highly complex "finite amplitude" theory. Eventually the breaking of waves presents a special problem, as yet inadequately approached. The effects of bottom resistance by friction and porosity also become more important with the "steepening" of the wave. In the following the effect of damping will be considered for very long, shallow water waves.

3.2 Transformation *with energy dissipation* for shallow water waves (2). Severe difficulties are encountered with the introduction of boundary friction into the general wave equations. Small amplitudes are assumed, and the resistance term must be linearized as first utilized by the prominent Dutch physicist H. A. Lorentz in planning the closure schemes of the Zuider Zee. The solution can then be stated for a channel of uniform depth with a maximum reference amplitude a_o (for $x = 0$) as a harmonic function:

$$\eta = a_o e^{-\mu x} \cos(\sigma t - k x) \tag{32}$$

μ represents a damping constant and the wave number k also is dependent on μ. Maximum amplitudes along x decrease exponentially. μ and k are related by:

$$\tan 2\alpha = \frac{f}{3\pi} \frac{u_o}{\sigma h} \tag{33a}$$

$$\tan \alpha = \frac{\mu}{k} \tag{33b}$$

$$k_o = \frac{\sigma}{\sqrt{gh}} = k \left[1 - \left(\frac{\mu}{k}\right)^2\right]^{1/2} \tag{33c}$$

hence all unknowns α, μ and k are defined by the quantities:

u_o = maximum velocity at the channel entrance

f = Darcy-Weisbach coefficient of resistance

h = channel depth

σ = tidal frequency = $\frac{2\pi}{T}$

$C_o = \sqrt{gh}$ = wave velocity without friction

The instantaneous velocity for any section is obtained for a given distance x from the entrance by:

$$u = \frac{a_o}{h} C_o e^{-\mu x} \frac{k_o}{\sqrt{\mu^2 + k^2}} \cos(\sigma t - k x + \alpha) \qquad (34)$$

The maximum value of u therefore also decreases with x as does the maximum value of η for any given x. The occurrence of the maximum velocity is displaced in time with respect to maximum tidal amplitude by a time angle α dependent on frictional effects. The wave velocity C is also reduced over the value $C_o = \sqrt{gh}$ since:

$$\frac{C}{C_o} = \frac{k_o}{k} = \frac{L}{L_o} = \frac{1}{\sqrt{1 + \left(\frac{\mu}{k_o}\right)^2}} \qquad (35)$$

For example, this ratio is for the: Delaware Estuary .94
Cape Cod Canal .91
WES Tidal Flume .78 to .80

It should finally be noted that in this approach valid for tidal wave phenomena the flow at any instant is assumed as a shear flow extending over the entire depth as in uniform flow in open channels. For shorter wave lengths certain boundary layer solutions for unsteady motion have been obtained, which should be referred to in reference (1).

B. Tidal Wave Characteristics in Estuaries

4.1 With the elements of wave theory developed toward the end of the last section various tidal wave problems may now be approached

analytically. For the general case, the basic differential equations of motion must be used directly since the cross sections may vary widely along the estuary channel. For this condition two methods of numerical analysis are available: numerical *integration by finite differences* (greatly aided now by computers) and solutions by the *method of characteristics* (3) (4) (5). The difficulty for both methods is primarily with the proper adjustment for friction effects and with results limited to tidal elevations and velocities. Extensive observations are therefore needed to check out the existing tides and then to proceed from there to predict the changes anticipated from engineering measures modifying the channel geometry or flow characteristics.

4.2 Whenever possible therefore, solutions by harmonic analysis are preferred which give general solutions for the entire estuary in terms of the basic wave components developed in equations (32) to (35) by superposition. Such solutions exist now for the Thames, Bay of Fundy (6) and the Delaware (7) estuaries. The method will be illustrated by application to the simple case of a rectangular tidal channel at the Waterways Experiment Station (8). The basic assumptions are:

a. A reference tide at the estuary mouth and complete reflection at the upstream end.
b. a (amplitude) $<$ h (depth) $<$ B (width) $<$ l (length of estuary).
c. Tidal wave length L is of the order of the length l of the estuary or larger.
d. Salinity variations and fresh-water flow give small velocities as compared to the tide.

Some estuaries show little variation in cross sections, others may be approximated by an exponential decrease in section to the tidal limit, where reflection takes place due to a dam or rapidly decreasing depth and width. In the WES flume complete reflection may be assumed as also proved acceptable for the Bay of Fundy and the Delaware. Since the damping constant μ must be the same for the incoming tidal wave and the reflected wave the equations of the combined system for a channel of constant depth and width are:

$$\eta = \eta_1 + \eta_2 = a_o \left[e^{-\mu x} \cos(\sigma t - kx) + e^{\mu x} \cos(\sigma t + kx)\right] \tag{36}$$

$$u = u_1 + u_2 = \frac{a_o C_o}{h} \frac{k_o}{\sqrt{\mu^2 + k^2}} [e^{-\mu x} \cos(\sigma t - kx + \alpha) - e^{\mu x} \cos(\sigma t + kx + \alpha)] \quad (37)$$

The constants can be evaluated from maximum tidal stage observations only as a function of x.

4.3 The results can be introduced into the energy balance at the estuary mouth, expressing the difference between the energy of the incoming and the reflected wave as the *energy dissipated* in the channel of length l. The average rate of dissipation per unit mass in the estuary is given by:

$$G = \frac{g C_o a_o^2}{hl} \frac{k_o}{\sqrt{\mu^2 + k_o^2}} \sinh 2\mu l \quad (38)$$

while the local rate of dissipation G_x may be expressed by the ratio:

$$\frac{G_x}{G} = \frac{1 - \frac{\sinh 2\mu x}{\sinh 2\mu l}}{1 - \frac{x}{l}} \quad (39)$$

The amplitude a_o represents here one half of the maximum tidal amplitude at the reflecting end of the estuary as observed. It may be replaced by the maximum tidal amplitude at the ocean end of the estuary η_{lH} from:

$$\eta_{lH} = a_o \sqrt{2(\cos 2kl + \cosh 2\mu l)} \quad (40)$$

It is seen that in addition to the geometric properties h and l only the existing stages need to be introduced from observations to define the damping terms, whereupon velocities and dissipation may be computed. This is the advantage of the harmonic analysis over the other methods, in which representative values of velocities and friction factors must be estimated. Further developments of this method for estuary sections exponentially decreasing from the mouth have been applied to the Delaware.

4.4 Extensive *experimental results* as well as field data confirm the value of the harmonic analysis. The tidal wave behavior in a rectangular channel was studied with this approach in order to check the

possible effects of salinity and of freshwater flow on the tidal velocities and stages. It was shown (8) (9) that the superposition of an incoming and reflected wave with proper damping coefficients as stated by equations (36) and (37) matched the experimental results with sufficient accuracy to warrant computation of tidal energy dissipation by equation (38). The influence of freshwater flow and of salinity remained of small consequence, however, it produced a slight rise in the mean level of the surface with the increase in these quantities toward the landward end of the channel. Damping factors μ were increased as expected from equation (33a) as the maximum computed tidal velocity u_o increased with amplitude a_o. Fig. 2 illustrates the entire set of results. The maximum tidal amplitudes at any station x are plotted here in terms of the maximum amplitude at the reflecting end of the channel (landward) versus the local time of high water measured again from the time of high water at the reflecting end. For any test (with constant amplitude of ocean tide) the points are close to a line of constant $\phi = 2\pi\left(\frac{\mu}{k}\right)$. This also illustrates the method of determining $\frac{\mu}{k}$ from the tidal observations. The primary value of the harmonic method lies in the possibility to predict changes in energy dissipation with tidal changes and will become evident from the following discussion on salinity intrusion.

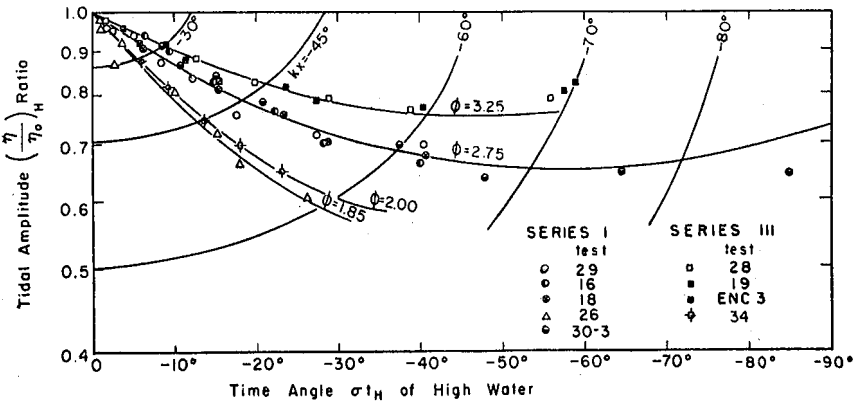

FIG. 2.—DETERMINATION OF DAMPING COEFFICIENT μ AND OF WAVE NUMBER k FROM TIDAL ELEVATIONS (8)

C. Salinity Intrusion in Estuaries

5.1 *The general problem of salinity intrusion* in tidal estuaries is one of extreme importance with respect to sedimentation and pollution. Two extreme cases may be illustrated by Fig. 3. The upper sketch shows the type referred to as "fully stratified" exhibiting a wedge of salt water, which remains unmixed with the fresh water flowing over it out to sea. The interface or boundary between the two layers is stable even though it may move slowly to and fro with the tides. In this country the Mississippi mouth contains such a salinity wedge. Its shape can be completely described and the length of intrusion can also be computed. The longitudinal pressure forces are indicated at the ends and give rise to a moment resulting in internal circulation within the wedge. Note, however, that the salt water flow Q_s must be compensating in downstream and upstream direction for a stationary wedge so that no net saltwater flow exists.

The lower sketch of Fig. 3 by contrast illustrates the extreme of salinity conditions at the opposite end of the spectrum. Severe tidal currents have generated sufficient turbulence to overcome the stabi-

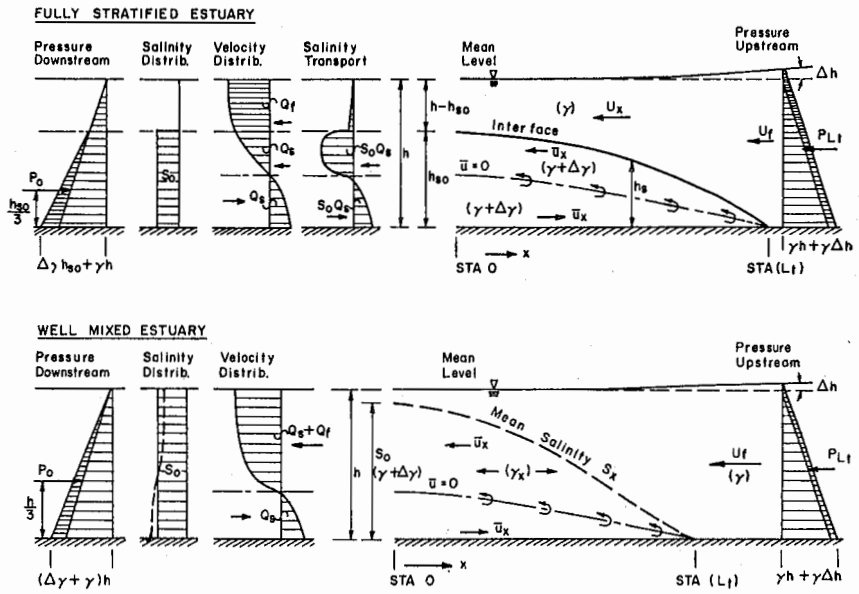

Fig. 3.—Schematic Representation of Salinity Intrusions in Estuaries (10)

lizing effects of the density difference and to produce a state of mixing between the salt and the fresh water which may be termed "well mixed," i.e., the vertical salinity differences are small. The sketch represents a state which is the result of looking at the time average of the current and salinity pattern rather than at the instantaneous patterns. The salinities are given as average salinities plotted vertically from the bottom and the average salinity varies from the maximum at the entrance section to zero at the toe of the intrusion. The static forces at the ends still produce upstream bottom velocities and a general circulation. Due to the mixing there is no "interface" as before, but a line of zero velocity (temporal mean) separates zones of adverse end of seaward flow. While it was shown in the preceding section that this temporal mean flow engendered by density differences has no effect on the much more intense tidal currents, the density underflow is of extreme importance for sedimentation. It retains all material settling into the bottom zones in the estuary, if it is too heavy to be lifted into the upper seaward flow. The presence of large amounts of silt in all estuaries is evidence of this mechanism and its detailed exploration is thus of extreme importance to the planning of engineering works in estuaries.

5.2 The *two-dimensional aspects of this internal circulation* may be illustrated by presenting the results of an experiment carried out in the WES tidal flume as analyzed at MIT (10). With an established tidal condition and freshwater flow, instantaneous velocity and salinity measurements were carried out at various stations from the ocean end at Sta. 5 (5 ft. from end) to Sta. 240 (240 feet from end). The velocity measurements were then averaged over several tidal cycles and plotted in Fig. 4 in terms of the mean freshwater velocity U_f against depth. The existence of strong upstream currents is apparent through Sta. 120 over a sizable portion of the section. Similarly, mean salinities are given in Fig. 5 in terms of the ocean salinity S_o versus depth exhibiting vertically an increase with depth and longitudinally decreasing values from Sta. 5 to Sta. 160. Large vertical gradients exist over the central portion of the intrusion length. These large gradients of salinity and hence density are responsible for the form of the distribution of horizontal velocities shown again in different form in Fig. 6. Values derived from Fig. 4 for various constant elevations in the stream are plotted versus distance and show maximum upstream components near the bottom between Sta. 40 and 80 and correspondingly strong downstream

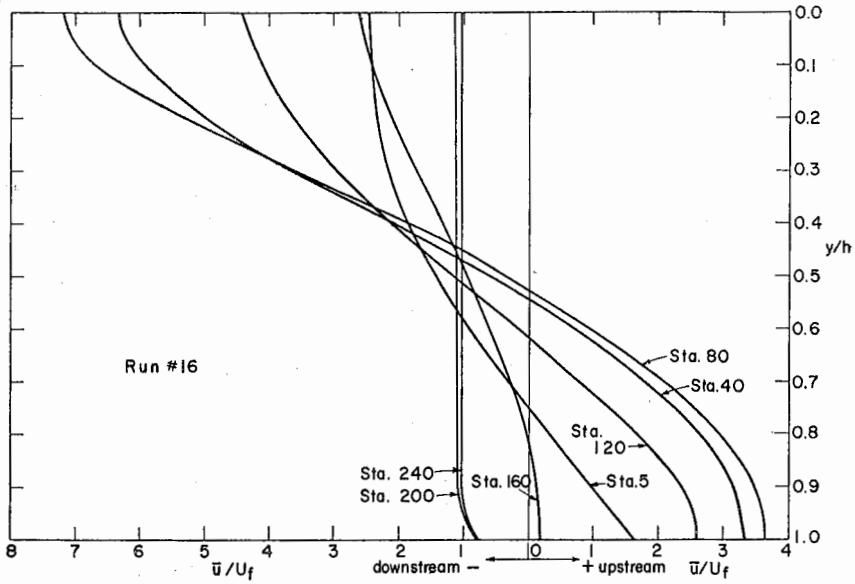

FIG. 4.—TIME-AVERAGE HORIZONTAL VELOCITY DISTRIBUTION (10)

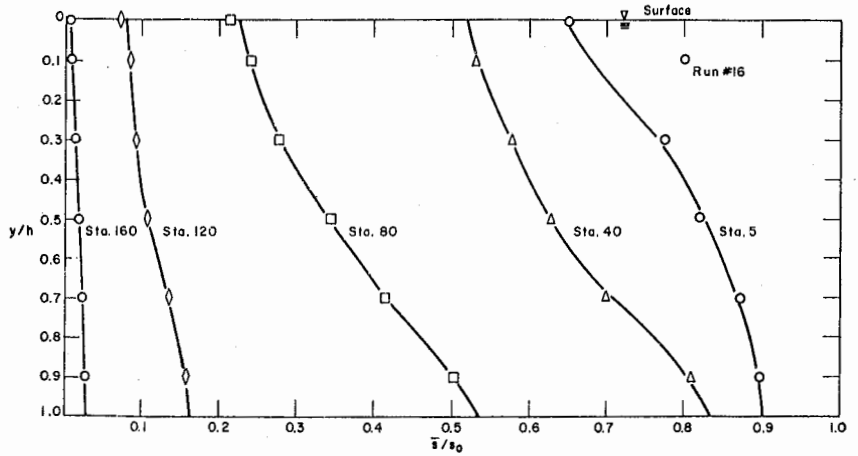

FIG. 5.—TIME-AVERAGE SALINITY/BASIN SALINITY (10)

velocities near the surface. This pattern of mean velocity distribution is related to the corresponding mean salinity profiles of Fig. 7, in which the strong longitudinal gradients of salinity between Sta. 40 and 80 are evident.

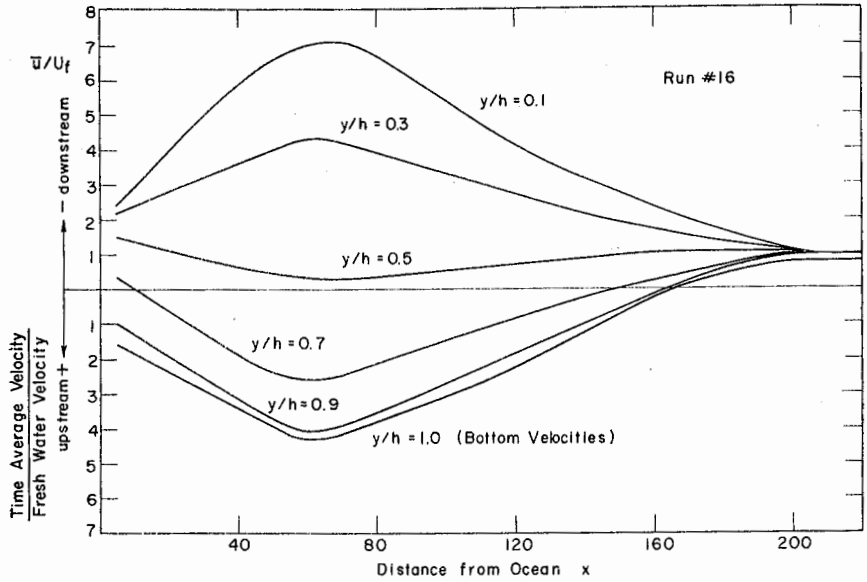

FIG. 6.—MEAN VELOCITIES ALONG CHANNEL AT VARIOUS DEPTHS (10)

Similar distributions, particularly of the typical velocity profiles of Fig. 4, have been observed in practice and have been presented by Simmons (11) as so-called "flow predominance curves." The correlation in many estuaries with shoaling patterns is obvious and has led to the planning of new techniques in coping with sedimentation in estuaries.

5.3 *One-dimensional solution of salinity intrusion.* Theoretical approaches on a two-dimensional basis to predict the behavior of salinity and internal velocities from the governing parameters of channel geometry, tidal wave motion, and freshwater flow are faced with as yet unresolved difficulties. The only assumption which leads to an approximate solution is the reduction of the general diffusion equation to a one-dimensional form, which eliminates the gradients of salinity in the vertical direction and considers uniform velocities over the vertical only. Salinity and velocity vary only with time and distance. The equation therefore reduces to the form:

$$\frac{\partial s}{\partial t} + (u_{x,t} - U_f)\frac{\partial s}{\partial x} = -\frac{\partial}{\partial x}(\overline{u's'}) = \frac{\partial}{\partial x}\left(D_x'\frac{\partial s}{\partial x}\right) \tag{41}$$

It is noted that the tidal velocity $u_{x,t}$ averages out to zero over a tidal cycle and the average salinity s will not change with time for constant U_f and constant tidal conditions. Therefore, averaging the equation with respect to time, the corresponding terms become zero and the equation reduces to:

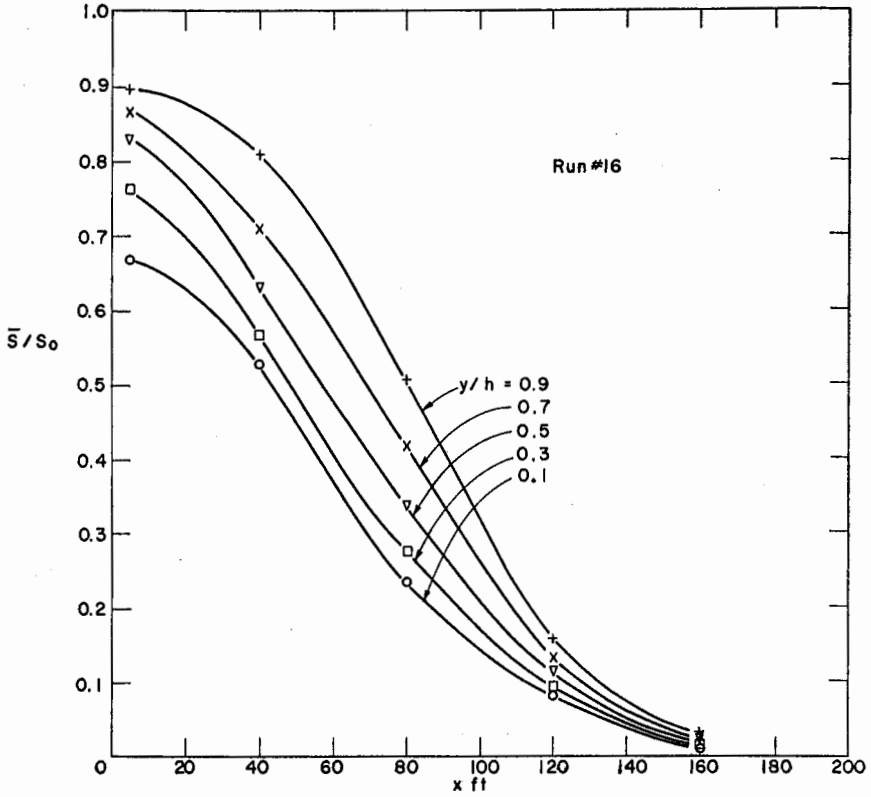

FIG. 7.—TIME-AVERAGE SALINITY VERSUS DISTANCE FROM OCEAN (10)

$$-U_f \frac{\partial \bar{s}}{\partial x} = \frac{\partial}{\partial x}\left(D_x' \frac{\partial \bar{s}}{\partial x}\right) \qquad (42)$$

This equation states that changes in the mean salinity due to U_f are prevented by the diffusion upstream of salinity due to the diffusion coefficient D_x' which embodies all turbulent and convective diffusion processes. The equation has been integrated (8) and put into the final

form describing the mean salinity distribution within the intrusion length *at low tide:*

$$-\ln\left(\frac{\bar{s}}{s_o}\right) = \frac{U_f}{2BD_o'}(x_l + B)^2 \tag{43}$$

This equation is based on the assumption that the diffusion coefficient D_x' is inversely proportional to distance from the ocean end, where it reaches a maximum value of D_o'. B is a constant to be derived from the observation of minimum values of $\bar{s}$ at low tide. Both constants D_o' and B are thus subject to definition from a few observations. It has also been shown that complete correlations can be obtained by relating D_o' to tidal energy dissipation G and the mixing energy rate J expended on the freshwater flow through the estuary. The expression for J is:

$$J = \frac{\Delta\gamma}{\gamma} g h \frac{U_f}{l} \tag{44}$$

Since G is given by equation (38) an empirical law has been established from all experimental results (see Figs. 8 and 9)

$$\frac{D_o'}{G^{1/3}} = 108\left(\frac{G}{J}\right)^{-1/2} \tag{45}$$

Hence the salinity distribution at low tide is completely described in terms of estuary geometry, tidal characteristics and freshwater flow. The salinity distribution for all tidal times is readily obtained by translating the low tide salinities with the tidal velocities obtained from the tidal analysis. For these solutions reference (8) is again to be consulted.

5.4 *Effects of salinity intrusion on sedimentation.* The effect of salinity in estuaries is twofold. On the one hand the internal dynamics are such as to produce a stagnation zone for the temporal mean velocities near the bottom thus retaining the sediments in the bottom zone near the end of the salinity intrusion. On the other hand the salinity promotes the flocculating of fine clay and silt and the much higher settling velocities of the flocs causes the fine suspensions coming from upland sources to accumulate in the bottom zones. The estuarine environment in addition provides fine suspended load due to entrainment by turbulence due to wave action on tidal flats and shallow portions of

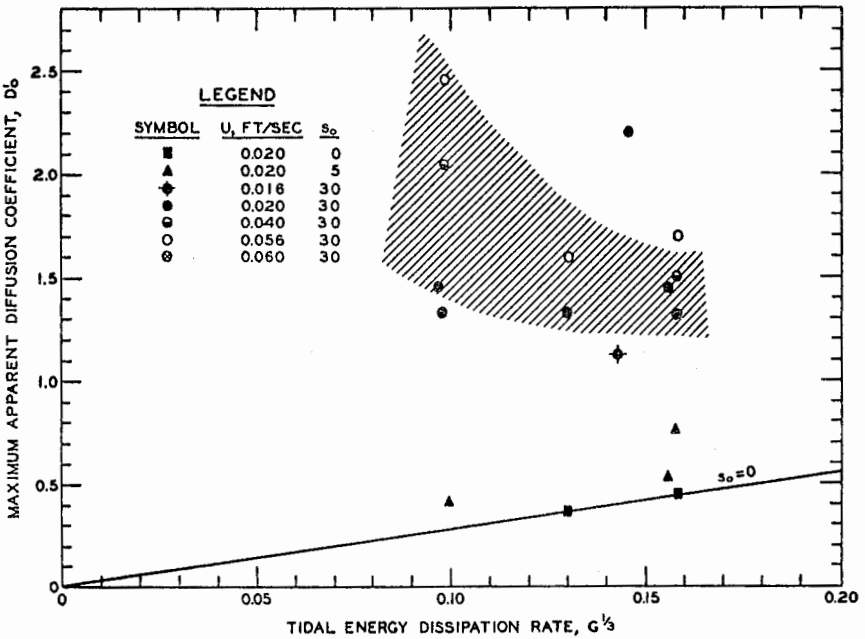

FIG. 8.—DIFFUSION COEFFICIENT VERSUS RATE OF TIDAL ENERGY DISSIPATION (8)

the estuary as well as from human and industrial sources. The *conclusions* from the internal dynamics of estuarine flow patterns are therefore:

1. Sediments reaching the bottom zones in estuaries will be transported upstream and not downstream.
2. Shoaling takes place primarily near the stagnation zones of the internal flow.
3. The higher the degree of stratification, i.e., the higher the salinity gradients both vertically and horizontally, the more intense is the shoaling.

General rules with regard to all engineering measures modifying the existing conditions are derived as follows:

a. The major portion of sediments in an estuary, if entrained by the periodic tidal velocities will be transported to the limits of the salinity intrusion. All measures leading to increasing depths and tidal range cause higher entraining velocities and thus promote localized shoaling.

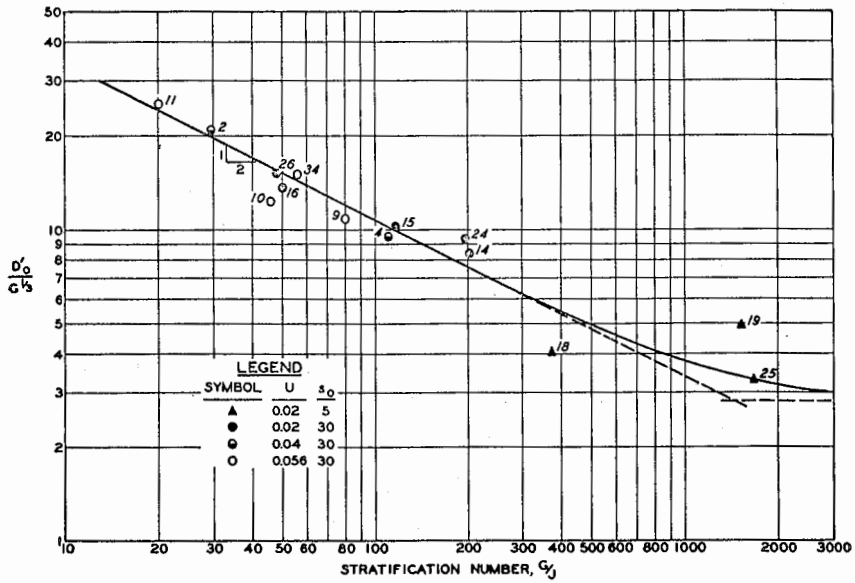

FIG. 9.—CORRELATION OF APPARENT DIFFUSION COEFFICIENT D_0' WITH STRATIFICATION NUMBER (8)

b. Engineering measures increasing normal freshwater flow by regulation or reducing tidal action by constriction lead to increased stratification and thus to increasing shoaling tendencies.

c. Dredging of navigation channels in estuaries should be accompanied by permanent removal of all dredge spoils from the estuaries. Dumping within the estuary confines back into the tidal streams is practically always useless. The criterion for dredging costs is not to be based on cost per cubic yard of dredging but on minimum annual costs of channel maintenance. In the case of the Delaware, complete removal of dredge spoils from the channel, while increasing the cost per cubic yard greatly, nevertheless produced a deeper channel year round for less annual cost of maintenance.

The definition of the *hydraulic characteristics of the shoaling materials* encountered in estuaries is a problem largely unresolved. Colloidal clays and fine sands of less than one quarter millimeter diameter are generally encountered as shoaling materials. The former constitute by far the predominant portion in all U. S. estuaries with

the exception of the Columbia River mouth. Colloidal clays will flocculate upon contact with saline water and due to the mean currents discussed before accumulate rapidly in shoals. These shoals become voluminous due to the small densities of only 1050 to 1200 grams per liter which only slowly consolidate due to the periodic disturbances by larger tides and large changes in fresh water flow. In general, the denser colloidal mixtures of water and clay-flocs have non-Newtonian characteristics as fluids, i.e., their initial displacement requires a finite shear and only for hydraulic shear forces in excess of this critical value will the mixtures behave as fluids. Needless to say the analysis of the complex interaction of sediment shoals and of the complicated flow regimes in estuaries is still only in the beginning stages and has led to extensive studies in the laboratory and in the field. The publications of the Tidal Hydraulics Committee of the Corps of Engineers (U.S. Waterways Experiment Station, Vicksburg, Mississippi) may be consulted with respect to progress made in this area, particularly with respect to planning of engineering works in San Francisco Bay.

It is hoped that this brief summary has at least produced an awareness of the complicated mechanics of estuary flow and sedimentation systems. Engineering measures interfering in this natural environment must be planned with full consideration of the organic interaction of tidal regime, freshwater flow, salinity and sediment characteristics.

References

1. Eagleson, P. S. and Dean, R. G. "Small Amplitude Wave Theory," Chapter A of "Estuary and Coastline Hydrodynamics," Hydrodynamics Laboratory, Department of Civil Engineering, MIT, 1963.
2. Ippen, A. T. and Harleman, D. R. F. "Tidal Dynamics in Estuaries," Chapter J of "Estuary and Coastline Hydrodynamics," Hydrodynamics Laboratory, Department of Civil Engineering, MIT, 1963.
3. Proudman, J. "Dynamical Oceanography," 1952, Methuen and Co., Ltd., London.
4. Dronkers, J. J. and Schoenfeld, J. C. "Tidal Computations in Shallow Water," Journal of the Hydraulics Division, ASCE, Separate No. 714, 1955.
5. Pillsbury, G. B. "Tidal Hydraulics," Revised edition 1956, Sales Agent, Superintendent of Documents, Waterways Experiment Station, Vicksburg, Miss.
6. Ippen, A. T. and Harleman, D. R. F. "Investigation of Influence of Proposed International Tidal Power Project on Tides in the Bay of Fundy," 1958 Report to New England Division, U.S. Corps of Engineers, Boston, Mass.
7. Goulis, D. "Damped Tides and Energy Dissipation in Exponential Estuaries with Particular Reference to the Delaware," 1962, S.M. Thesis, MIT, Department of Civil Engineering.
8. Ippen, A. T. and Harleman, D. R. F. "Analytical Studies of Salinity Intrusion in Estuaries and Canals," 1961, Committee on Tidal Hydraulics, Corps of Engineers, Technical Bulletin No. 5.

9. IPPEN, A. T. "Salinity Intrusion in Tidal Estuaries," Chapter M of "Estuary and Coastline Hydrodynamics," Hydrodynamics Laboratory, Department of Civil Engineering, MIT, 1963.
10. IPPEN, A. T. AND HARLEMAN, D. R. F. "Two-Dimensional Aspects of Salinity Intrusion in Estuaries," 1964, Committee on Tidal Hydraulics, Corps of Engineers, Vicksburg, Miss.
11. SIMMONS, H. B. "Some Effects of Upland Discharge on Estuarine Hydraulics," Proc. ASCE, Separate No. 742, 1955.

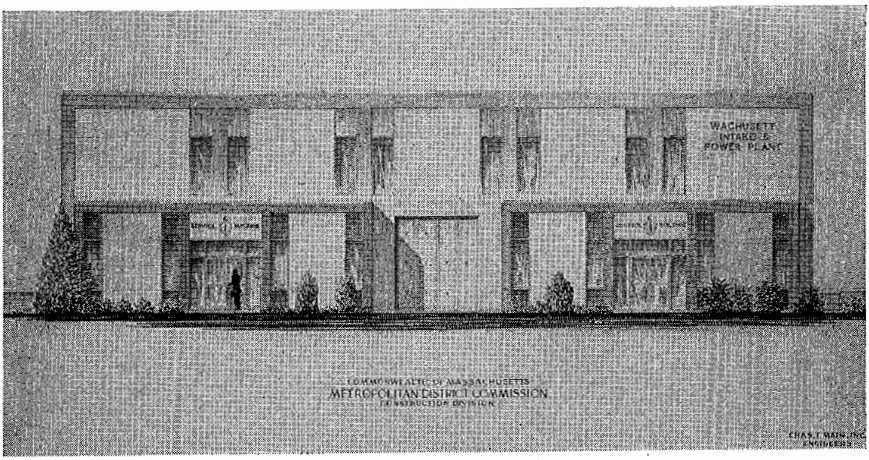
WACHUSETT
INTAKE &
POWER PLANT
COMMONWEALTH OF MASSACHUSETTS
METROPOLITAN DISTRICT COMMISSION